



## STRENGTHENING OF CONCRETE BEAMS WITH PRESTRESSED FRP REINFORCEMENTS

Dr. Suhaib Sabah Abdulhameed

Lecturer Civil Engineering Department, Mustansiriyah University, Baghdad, Iraq.

**Abstract:** Strengthening of reinforced concrete beams with prestressed Fiber Reinforced Polymer (FRP) sheets showed to be efficient in enhancing the serviceability of the strengthened concrete beams. Yu et al.'s develop a mechanical prestressing device to prestress FRP sheets to strengthen reinforced concrete members. Yu et al. s experimental results showed that this device overcome the shortcomings associated by using the previously developed prestressing devices. In this research program Yu et al.'s mechanical device was modified to increase the efficiency of it by using light weight material to reduce the additional weight on the strengthened beams caused by the prestressing device in addition, the end anchorage plates were installed vertically rather than horizontally to extend the prestressed FRP sheets to the end regions of the member where high shear stress occurred. This modification in the end anchorage regions is efficient to reduce the possibility of the premature debonding failure. A numerical analysis by using ANSYS (R14.5) computer program was used to simulate the prestressing device. Numerical results showed that using aluminum material is efficient to produce a prestressing mechanical device. The maximum stresses and deflection that generated in the prestressing device upon prestressing Carbon Fiber Reinforced Polymer (CFRP) sheet (51% of the ultimate tensile stress in the CFRP) to strengthen 22.5m concrete beam are 46MPa and 83mm respectively. A theoretical formula was derived based on geometric relations of the prestressing system and the deformed CFRP sheet. It was used to predict the prestressing level in the CFRP sheet. Theoretical results showed that the percentage difference between Yu et al.'s formula and the derived formula is about 1%. This value changes based on the prestressing level in CFRP sheet and the length of the strengthened beam. The theoretical prediction of prestressing level in the CFRP sheet agreed well with the experimental results.

**Keywords:** CFRP sheet, finite element analysis, Ansys computer program, prestressing device

### تقوية الجسور الخرسانية باستخدام اليااف الفايبر المسبقة الجهد

**الخلاصة:** ان طريقه تقويه العناصر الخرسانية باستخدام اليااف الفايبر المسبقة الجهد من الطرق الحديثه لما لها من تاثير على سلوك العناصر الخرساني قبل وبعد اجراء اعمال التقويه. تم تصنيع جهاز الي من قبل الباحثين (Yu et al.) لتسليط اجهادات مسبقه الجهد على اليااف الفايبر قبل اجراء التقويه للعناصر الخرسانية. تم اجراء فحوصات مختبريه لفحص كفاءه الجهاز من قبل الباحثين Yu et al. اظهرت النتائج العمليه بان الجهاز المصنع كفوء وعلمي في تسليط اجهادات مسبقه الجهد على اليااف الفايبر. تم استعمال برنامج التحليل ANSYS R14.5 لاعاده تصميم الجهاز وبما يزيد من كفاءته وسهوله استخدامه. اهم المتغيرات التي اعتمدت في تصميم الجهاز هو استعمال مواد خفيفه الوزن (الالمنيوم) في تصنيعه مما يقلل الاجهادات على الجسور الخرسانية، كما تم تثبيت طرفي اليااف الفايبر عموديا قبل اجراء اعمال السحب مما يقلل احتماليه الفشل المبكر للجسور الخرساني المقوى عند تعرضه للاحمال الخارجيه وخاصه في منطقه القص. اظهرت النتائج النظرية بان الاجهادات والهطول الكلي الذي يحصل في الجهاز عند تقويه 22.5م طول للجسر الخرساني هو 46 ميكا باسكال و 83ملم بالتعاقب. تم اشتقاق معادله رياضيه تستعمل لحساب الاجهادات المراد تسليطها في اليااف الفايبر دون الحاجه لاستعمال اجهزه الكترونيه مما يساعد على اختصار الوقت والكلفه عند اجراء اعمال التقويه حقليا".

## 1. Introduction

Strengthening of reinforced concrete beams with prestressed carbon fiber reinforced polymer (CFRP) sheets showed to be efficient due to the superiority of this technique in enhancing the serviceability of the strengthened beam and control of cracks by reducing crack widths and delay the onset of cracking.

Many researchers developed prestressing systems to prestress FRP sheets to strengthen reinforced concrete members [1-6]. The shortcomings associated by using the previously developed prestressing systems are: 1) appropriate to use in the laboratory more than in site application, 2) hydraulic jacks are used to apply prestress in the FRP sheet, 3) the FRP sheet cannot extended along the length of the strengthened beams, and 4) releasing of the FRP sheets occurred under high strain rate which may lead to premature debonding failure [7].

To overcome the shortcomings associated by using the previously developed systems, Yu et al [7] developed a mechanical prestressing device that is used to prestress CFRP sheets. The main characteristic of this device are: the ends of the CFRP sheets are directly fixed to the device, the prestressing force are applied manually, and transferring of the prestress force occurred under slow strain rates.

The shortcomings accompanied by using Yu et al's device is that the weight of the device increases with an increasing the length of the strengthen beams causing to increase the stresses on the precracked strengthened beams, in addition the pestressed CFRP sheets can't be extended to the end region of the concrete member . Accordingly the prestressing device can be modified to increase the efficiency of it and to overcome the shortcomings.

Fig. 1 shows the geometrical shape and dimensions of Yu et al's pretressing device. This device is divided into segments. These segments were divided based on the geometric relations of the prestressing system and the deformed CFRP sheets. Segment 1 ( $L_1$ ), Segment 2 ( $L_2$ ), and segment 3 ( $\Delta H$ ) which is measured directly from the device based on the length of the strengthened beams and the prestressing level.

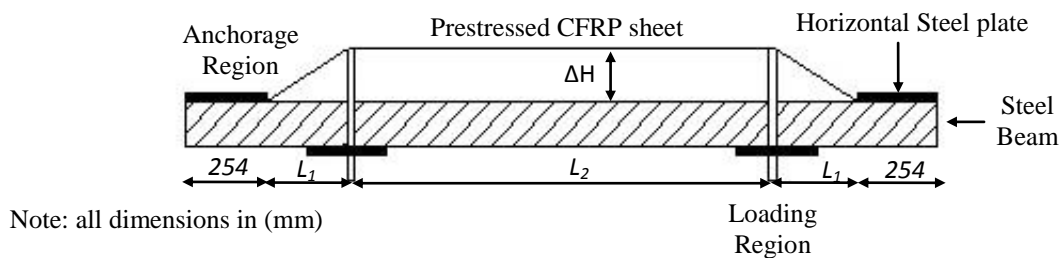


Figure 1. Mechanical prestressing device to prestress CFRP sheets [7].

A Finite Element Analysis (FEA) simulation by using ANSYS (R14.5) computer program was used to analysis the mechanical device with prestressed CFRP sheets. In this research program, the numerical simulation was divided into two groups. The first group consist of calibration of the numerical models with the experimental results, while the second group consist of modification of the prestressing device. A theoretical formula was derived to predict the prestressing level in the CFRP sheet.

## 2. ANSYS Finite Element Model

The FEA calibration study included modeling a mechanical steel device with the dimensions and properties corresponding to mechanical device developed by Yu et al (2008).

To create the finite element model in ANSYS, there are multiple tasks that must be completed for the model and to run it properly. This model was created using command prompt line input. This section describes the different tasks and entries that were used to create the FE calibration model.

### 2.1 Element Type

In this analysis two elements were used to simulate WT8x18 section, steel plates, and CFRP sheet. These elements can be summarized as follows:

1. An eight-node solid element, solid45 was used to simulate the WT section and steel plates. The element is defined with eight nodes having three degrees of freedom at each node, translations in the nodal x, y, and z directions [8]. The element has plasticity, creep, swelling, stress stiffening, large deflection, and large strain capabilities. A schematic diagram of the element is shown in Fig. 2.

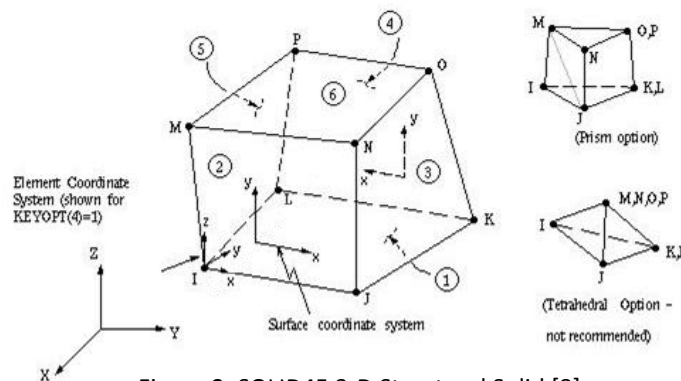


Figure 2. SOLID45 3-D Structural Solid [8].

2. The three dimensional spar element (Link8) was used to simulate the CFRP sheet. Two nodes are required for this element. Each node has three degrees of freedom, translations in the nodal x, y, and z directions [8]. This element is shown in Fig. 3.

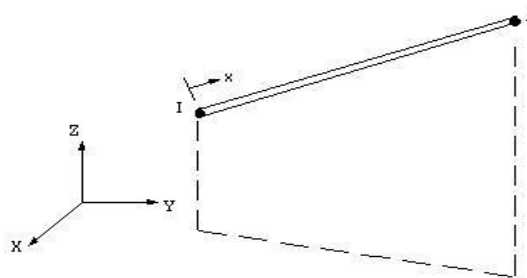


Figure 3. LINK8 3-D Spar [8]

The prestressing effect on the CFRP sheet was applied to the model by providing initial strain (ISTRN). The effect of nonlinearities was included in the analysis by using bilinear isotropic hardening to ensure that yielding of steel will not occur in the device when the prestressing force is applied.

## 2.2 Real Constants

The real constants for this model are shown in Table 1. No real constant set exists for the Solid45 element. Real Constant Sets 2 is defined for the Link8 element. Values for cross-sectional area and initial strain were entered

Table 1. Real Constants for Calibration Model.

Real constant set	Element type		Real constant value
2	Link8	Cross-sectional Area (mm <sup>2</sup> )	1.19/ply
		Initial Strain	15% $\epsilon_{fu}$ , 30% $\epsilon_{fu}$ , 40% $\epsilon_{fu}$

## 2.3 Material Properties

Parameters needed to define the material models can be found in Table 2. As seen in this table, there are multiple parts of the material model for each element.

Table 2. Material Models for the Calibration Model.

Material Model Number	Element type		Real constant value
1	Solid45	Modulus of elasticity GPa	200
		Poisson's ratio	0.3
		Yield stress MPa	350
2	Link8	Modulus of elasticity GPa	228
		Poisson's ratio	0.3
		Ultimate stress MPa	3790

## 2.4 Modeling

The WT beam and plates were modeled as volumes. Table 3 summarized the main dimensions of steel plates and WT beam.

Table. 3 main dimensions of the mechanical device components

Components name	Components ID	Dimensions (mm)
Removable plate	A	279X254X9.5
Welded plate	B	279X254X9.5
Loading region plate	C	180X500X10
Mid-span plate	D	180X900X10
WT 8 x18 section	E	178X201

The combined volumes of the WT and plates are shown in Fig. 4. The FE mesh for the beam model is shown in Fig. 5. As shown from this figure, the number of elements equal to 50077. It's worth to mention that the procedure for modeling, meshing, and analysis of the device are available in Basic Analysis Guide of ANSYS manual, Modeling and Meshing Guide of ANSYS manual, and Structural Analysis Guide of ANSYS manual [8].

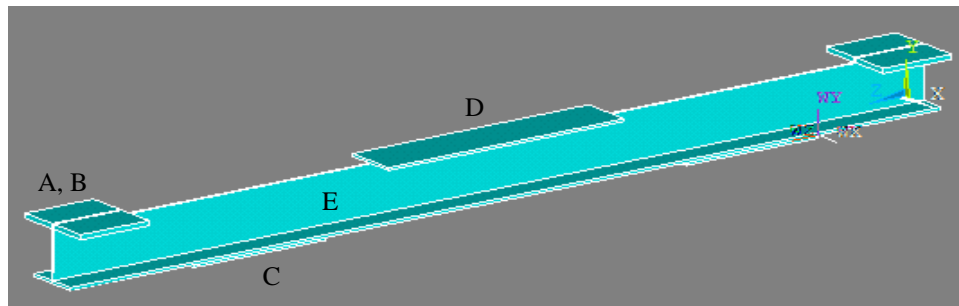


Figure 4. Volumes Created in ANSYS.

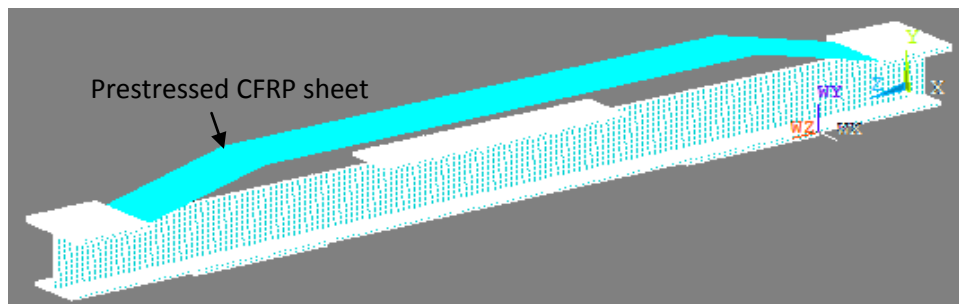


Figure 5. FE meshing of the steel device.

## 2.5 Calibration of the Material Model

To verify the validity of the model and analysis, a comparison between numerical and experimental results was carried out of three prestressing level (15%, 30%, and 40% of the ultimate tensile stress of CFRP sheet ( $f_{tu}$ )) based on the experimental results done by Yu et al [7].

In this analysis, the length of the strengthened beam is 2440mm,  $L_1$  equal to 457mm, and  $L_2$  equals to 1990mm based on Yu et al's device.

Fig.6 shows the normalized prestressing stress versus the vertical displacement of the experimental and numerical results. As shown from this figure, the numerical results well agreed with the experimental results.

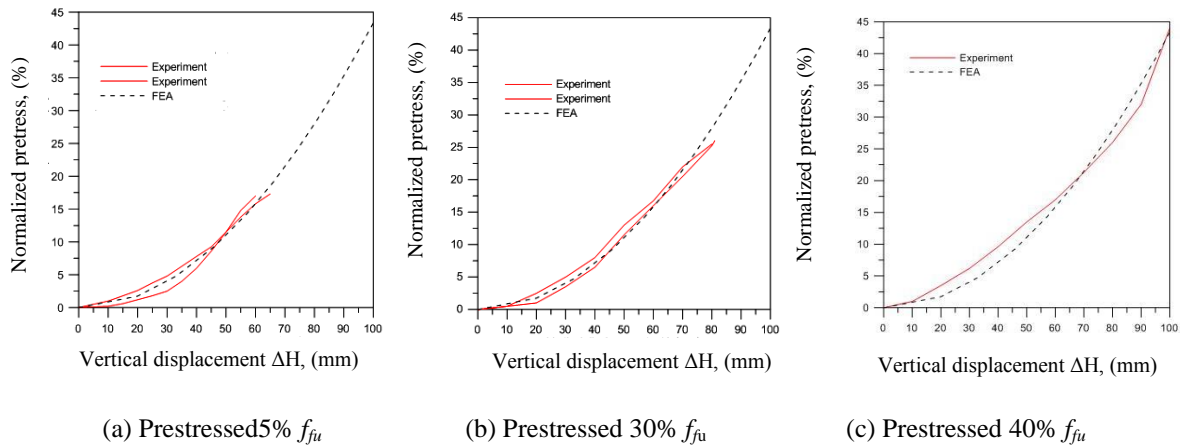
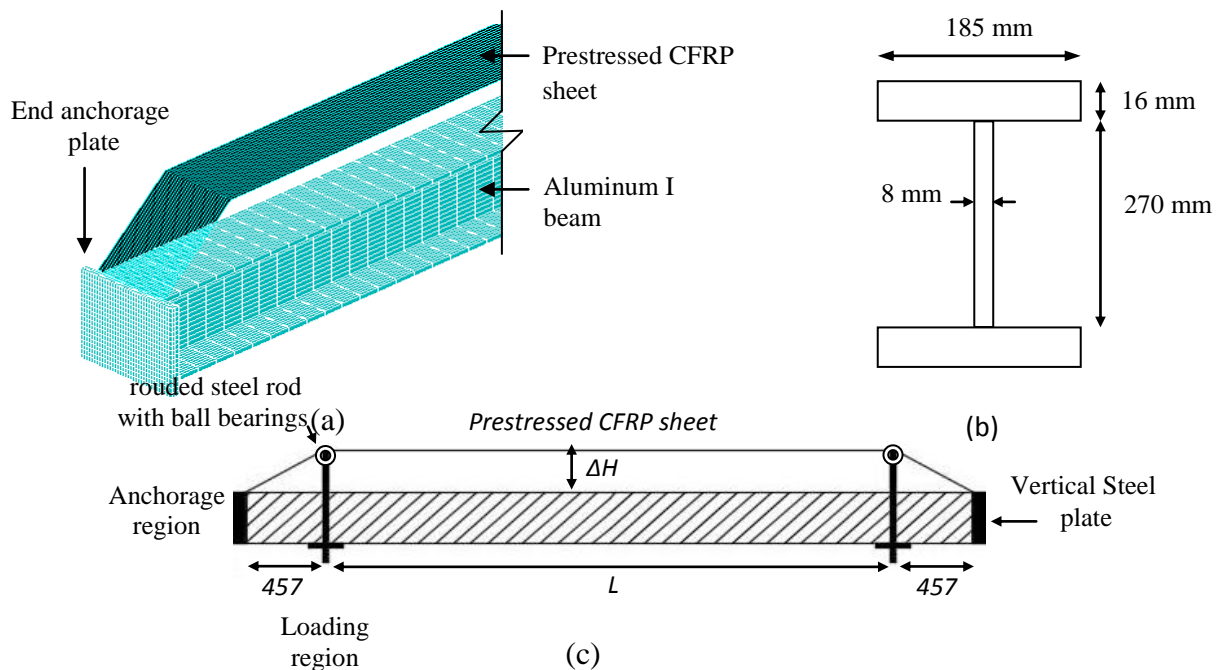


Figure 6. Comparison between numerical and experimental results.

### 3. Design Modification of Mechanical Prestressing Device

In order to overcome the shortcomings of Yu et al.'s device, a light weight material (aluminum material) can be used instead of steel material to produce the prestressing device (aluminum density equal to about 30% of the steel density). In this analysis, the main modification of Yu et al.'s device is: 1) using aluminum material to reduce the weight of the device especially for long retrofitted beams, 2) the end anchorage plates were installed vertically rather than horizontally to extend the prestressed FRP sheets to the end regions of the member. Fig. 7 shows the five segments of mechanical device that was used in this analysis. The length of  $L_1$  is kept constant 457 mm, while the length of  $L_2$  is determined based on the length of the strengthened beam. In this analysis  $L_2$  equals to 21.6 m to strengthen 22.5 m concrete beam as shown in the schematic diagram.



Note: all dimensions in mm

Figure 7. a) FEM discretization for prestressing mechanical device, b) main dimensions of I Beam, (c) Schematic diagram of mechanical device.

The prestressing effect on the CFRP sheet was applied to the model by providing an initial strain across (51%  $f_{fu}$ ). This value is lower than the permissible limit (55%  $f_{fu}$ ) based on the recommendation of ACI Committee 440(2008) [9], after consideration of a long-term environmental factor (creep-rupture), which for carbon fibers not exposed to weather is  $C_E=1$ , and the sustain stress limit for the CFRP sheets is 55%  $f_{fu}$ .

Tables 4 and 5 show the material properties of the aluminum I beam (6061-T6) and CFRP sheet respectively that was used in this analysis.

Table 4. Material properties of Aluminum I beam (6061-T6)

Density	2.7g/cm <sup>3</sup>
Ultimate tensile strength	310MPa
Tensile yield strength	276 MPa

Table 4. Material properties of Aluminum I beam (6061-T6)

Elongation at break	12%
Modulus of elasticity	68.9 GPa
poisson's ratio	0.33
Shear modulus	26GPa

Table. 5 Material properties of CFRP sheet

Ultimate tensile strength	3790MPa
Ultimate strain	1.7%
Elastic modulus	228GPa
Area	(0.165mm)thick x (200mm) wide =33mm <sup>2</sup>

Fig. 8 shows the von-mises stress that generated in the aluminum device. Upon applying a prestressing force, the maximum stress equal to 46 MPa, this value is lower than the yielding stress of the aluminum (276 MPa).

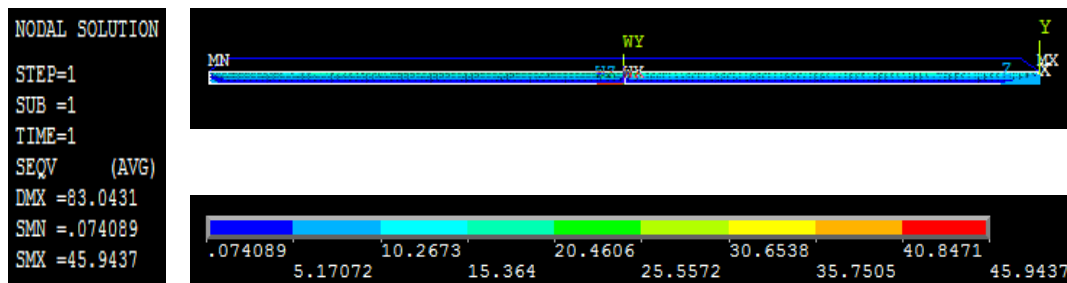


Figure 8. Von mises stresses in the prestressing device.

Fig. 9 shows the von - mises stresses that generated at the end anchorage region (part a) and in the mid span region (part b) of Fig. 8. As shown from these figures the

higher stresses generated at the end anchorage region especially at the points of contact between WT section and the anchorage plates

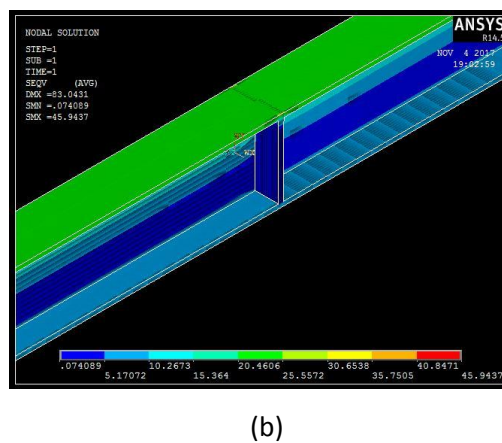
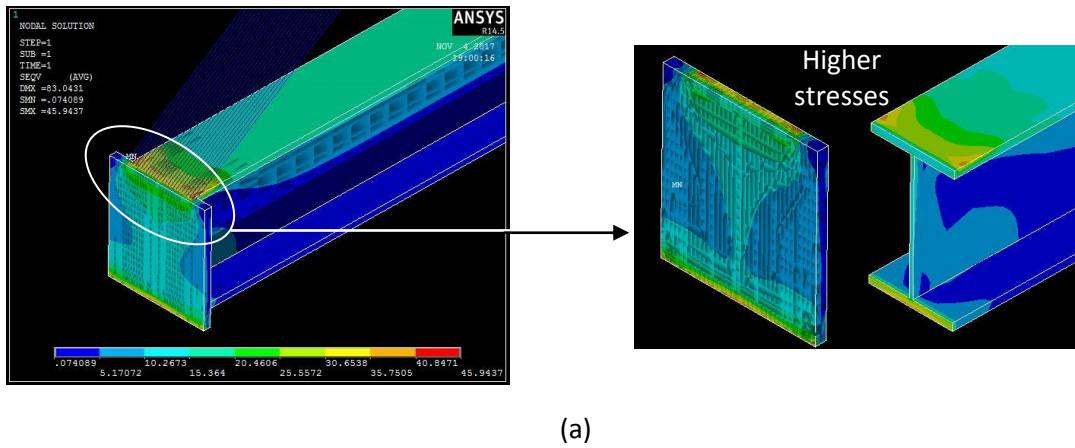
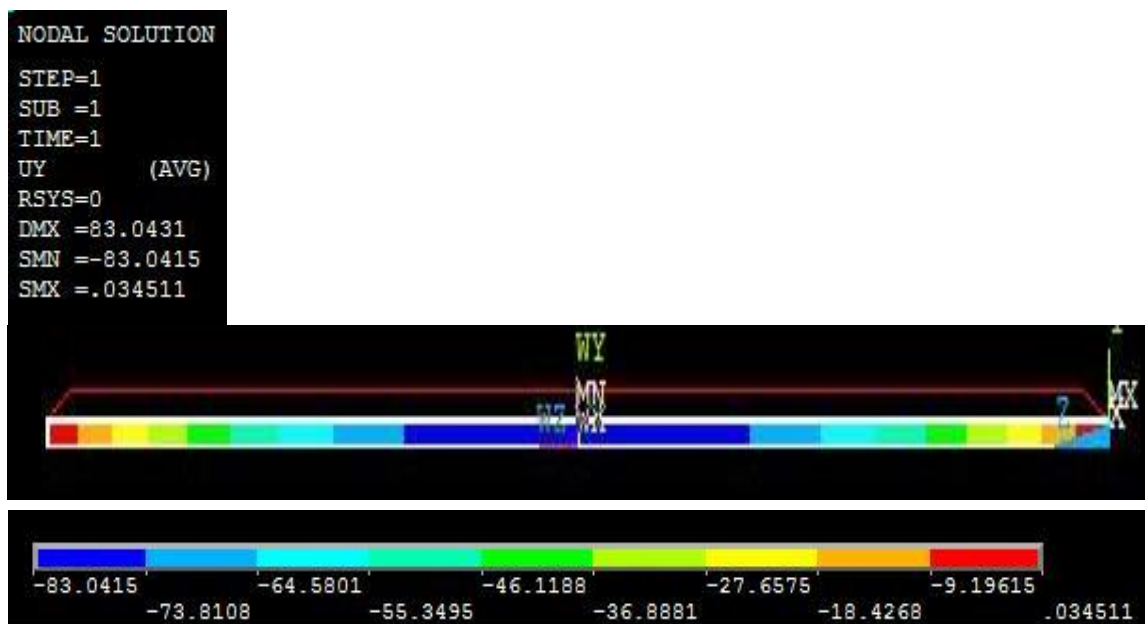


Figure 9. Von mises stresses in the prestressing device (a) end anchorage region, (b) Mid span region.

Fig. 10 and Fig. 11 show the displacement in the Y direction. As shown from this figure, the maximum displacement in the mid-span region is 83mm.





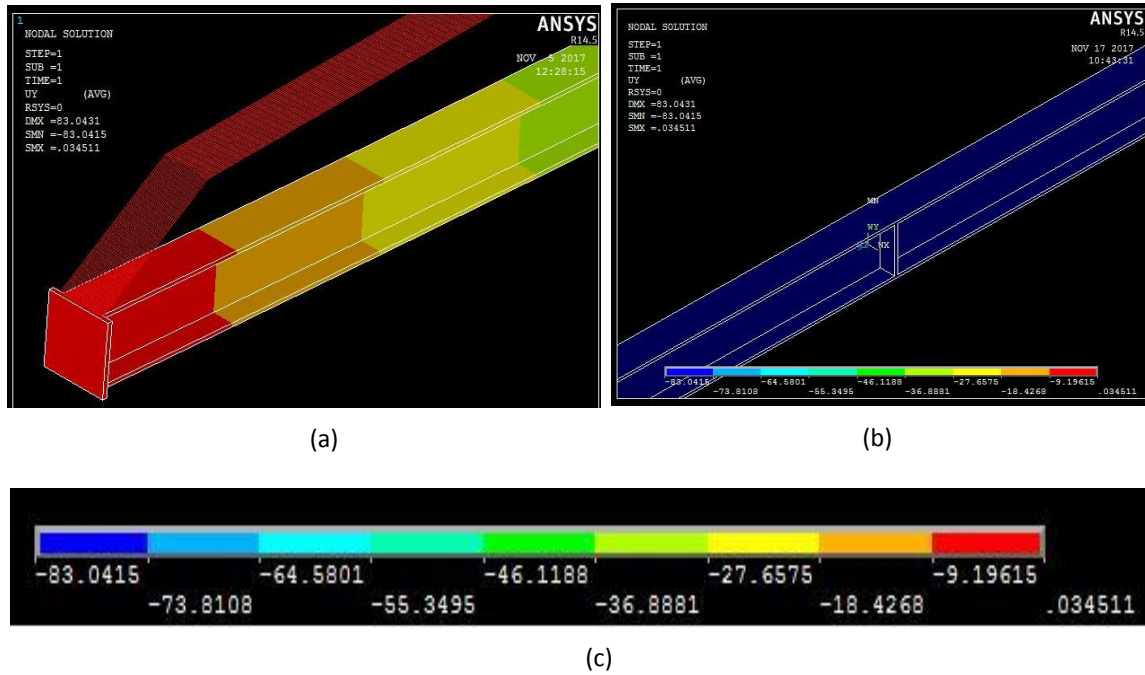


Figure 11. (a) Displacement in the end anchorage region; (b) Displacement in the mid-span region; (c) Displacement gradient in the Y-direction along the length of the mechanical device.

Fig.12 shows the normalized prestressing stress versus the vertical displacement in the mid-span region of the Aluminum device. As shown from this figure, by prestressing the CFRP sheet to 51%  $f_{fu}$ , the maximum displacement in the mid-span region increased to about 83.0415mm.

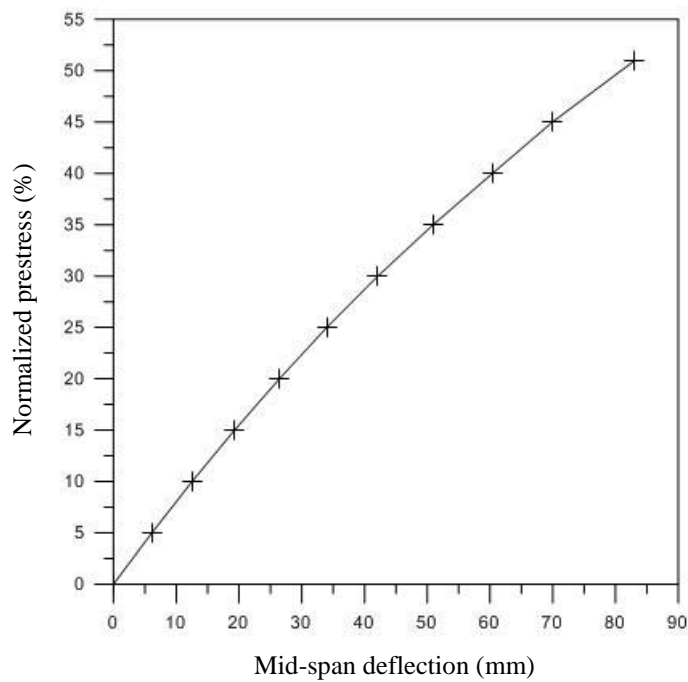


Figure 12. Normalized prestress versus mid span deflection of aluminum device

Fig. 13 shows that the maximum stress in the end anchorage region increased linearly to about 46 MPa when the initial stress in the CFRFP sheet equal to about 51%  $f_{fu}$

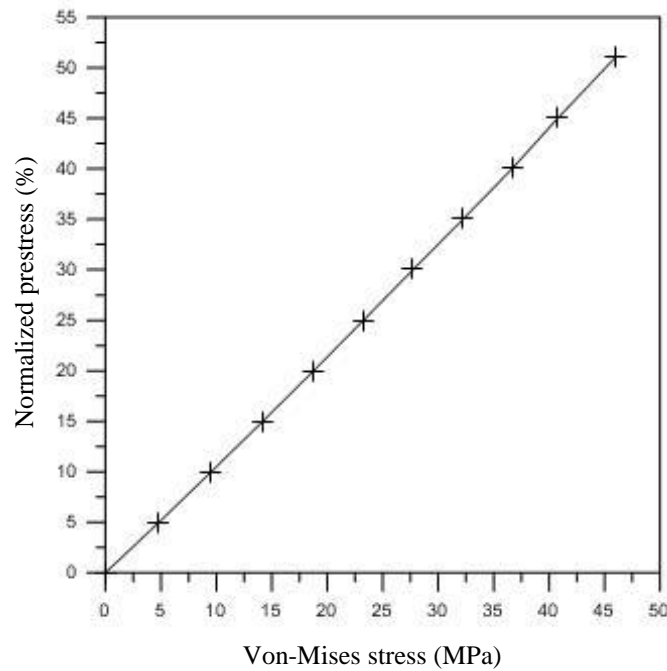


Figure 13. Normalized prestress versus Von-Mises stress of aluminum device.

Based on the numerical results, it was observed that the stresses that generated in the prestressing device are within the acceptable limits.

#### 4. Theoretical Prediction of Prestressing Level in CFRP Sheet

Yu et al (2008) [7], derived a theoretical formula to evaluate the prestress in CFRP sheet based on the geometric relations of the prestressing system and the deformed CFRP sheet as shown in Fig. 14.

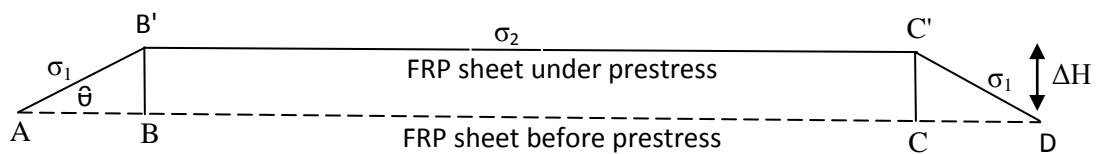


Figure 14. Schematic diagram of prestress and non prestress profile in CFRP sheet.

The theoretical formula is:

$$\frac{\sigma_2}{f_{fu}} (\%) = \frac{2L_1(\sqrt{L_1^2 + \Delta H^2} - L_1)}{L_1L_2 + 2(L_1^2 + \Delta H^2)} \frac{E_f}{f_{fu}} \times 100\% \quad (1) \quad \text{(Yu et al.'s formula)}$$

Where  $\sigma_1$  and  $\sigma_2$  are the stresses in segments AB' and BC' respectively, and  $E_f$  is the modulus of elasticity of CFRP.

The relation between  $\sigma_1$  in the segment (AB') and  $\sigma_2$  in the segment (B'C') was expressed as:

$$\sigma_2 = \sigma_1 \cos\theta \quad (2)$$

As shown in Fig. 6, the value of  $\theta$  are  $7.85^\circ$ ,  $9.93^\circ$ , and  $12.3^\circ$  for  $\Delta H$  equal to 63mm (Fig.6a), 81mm (Fig.6b), and 100mm (Fig.6c) respectively ( $L_1=457$ mm). If the angle  $\theta$  (refer to Fig.14) increased from zero to 90 degree (based on equation 2), then the value of prestressing force ( $\sigma_2$ ) in the segment (B'C') was reduced to zero. Based on the Newton's laws of motion and the linear behavior of CFRP sheet, the prestressing stress in the CFRP sheet in all segments are equal, then the theoretical formula can be re-derived as follows

$$\sigma_2 = \sigma_1 \quad (3)$$

$$\Delta L = \frac{\sigma_2 L_2}{E_f} + \frac{2\sigma_1}{E_f} \sqrt{L_1^2 + \Delta H^2} = 2(\sqrt{L_1^2 + \Delta H^2} - L_1) \quad (4)$$

Where  $\Delta L$  is the elongation in the CFRP sheet

Substitute equation 3 into equation 4, the prestressing stress ( $\sigma_2$ ) in the segment B'C' can be expressed as:

$$\sigma_2 = \frac{2E_f(\sqrt{L_1^2 + \Delta H^2} - L_1)}{(L_2 + 2\sqrt{L_1^2 + \Delta H^2})} \quad (5)$$

The normalized prestress ( $\frac{\sigma_2}{f_{fu}}$ ) is:

$$\frac{\sigma_2}{f_{fu}} (\%) = \frac{2(\sqrt{L_1^2 + \Delta H^2} - L_1)}{(L_2 + 2\sqrt{L_1^2 + \Delta H^2})} \frac{E_f}{f_{fu}} \times 100\% \quad (6)$$

Table 6 shows the normalized prestress that was determined based on equations 1 and 6. As shown from this table, the percent difference between equations 1 and 6 is about 1%. This value changes based on  $L_1$ ,  $L_2$  and the prestressing level.

Table 6. Normalized prestressing in equations 1 and 2

Modulus of elasticity of CFRP Gpa	Ultimate tensile stress Mpa	L1 mm	L2 mm	$\Delta H$ mm	Prestressing level %	Eq. 1 %	Eq.6 %	% difference
228	3790	457	1900	110	55	54.8	55.3	1

Fig. 15 shows the comparison between the experimental and theoretical results. As shown from this figure, theoretical prediction of the prestressing level in the CFRP sheet agreed well with the experimental result.

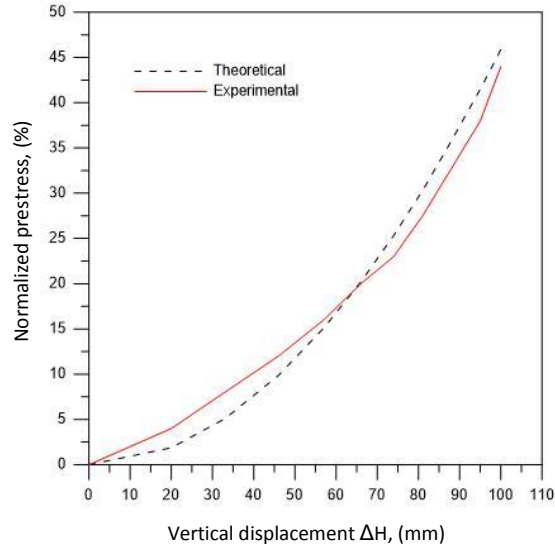


Figure 15. Comparison between experimental and theoretical results.

## 5. Conclusions

The main conclusions of this investigation can be summarized as follows:

- 1- Using Aluminum material can be used efficiently to produce a prestressing mechanical device.
- 2- The end anchorage plates can be installed vertically rather than horizontally to extend the prestressed FRP sheets to the end regions of the concrete member where high shear stress occurred.
- 3- The maximum stress that generated in the Aluminum device upon prestressing CFRP sheet is equal to 46 MPa, this value is lower than the yielding stress of the Aluminum (276 MPa).
- 4- The maximum displacement in the mid-span region of the prestressing device is 83mm for 22.5m concrete beam.
- 5- The percent difference between the derived formula and Yu et al.'s formula is about 1%. This value changes based on  $L_1$ ,  $L_2$  and the prestressing level.
- 6- The theoretical prestressing level in the CFRP sheet agreed well with the experimental results.

## 6. References

1. Triantafillou, T. C., Deskovic, N., and Deuring, M. (1992). "Strengthening of Concrete Structures with Prestressed Fiber Reinforced Plastic Sheets." *ACI Struct. J.*, 89 (3), 235- 244.
2. Quantrill, R. J., and Hollaway, L. C. (1998). "The Flexural Rehabilitation of Reinforced Concrete Beams by the Use of Prestressed Advanced Composite Plates." *Compos. Sci. Technol.*, 58, 1259 - 1275.
3. Garden, H. N., Hollaway, L. C. (1998), "An experimental study of the failure modes of reinforced concrete beams strengthened with prestressed carbon composite plates." *Composites Part B*, Vol. 29B, 411 - 424.

4. Wu, Z., Matsuzaki, T., Yokoyama, K., and Kanda, T. (1999). *"Retrofitting method for reinforced concrete structures with externally prestressed carbon fiber sheets."* Proc., 4<sup>th</sup> Int. Symp. on Fiber Reinforced Polymer Reinforcement for Reinforced Concrete Structures, , PRPRCS-4, Baltimore, Maryland, 751 - 765.
5. Huang, Y., Wu, J., Yen, T., Hung, C., and Lin, Y. (2005). *"Strengthening reinforced concrete beams using prestressed glass fiber-reinforced polymer – part I: experimental study."* J. Zhejiang University Science, 6 (3), 166 - 174.
6. Meier, U. (2000). *"Multifunctional Materials in Structural Engineering. Keynote Lecture at the advanced Composite Materials in Bridges and Structures."* Conference, (ACMBS III). Ottawa, Canada. August 15 - 18, 2000.
7. Yu, P., Silva, PF, and Nanni, A. (2008). *"Description of a Mechanical Device for Prestressing of Carbon Fiber Reinforced Polymer Sheets."* Part I. ACI Struct. J., 105 (1), 3 - 10.
8. ANSYS user's manual, version 8.0 Houston, Texas: Swanson Analysis systems Inc. (SASI), 2004.
9. ACI 440.2R-08, Guide for the Design and Construction of Externally Bonded FRP Systems for Strengthening Concrete Structures, American Concrete Institute, Farmington Hills, MI, USA, 2008.